Aspects of a hybrid hp-finite element/spectral method for the linearised magnetohydrodynamic equations in spherical geometries

D. Farmer[1] D. J. Ivers[2]

(Received 30 January 2011; revised 28 June 2011)

Abstract

We consider the incompressible magnetohydrodynamic equations, linearised about a steady basic state in spherical geometries. The angular dependence is discretised using a Galerkin method based on spherical harmonics. This produces a coupled system of ordinary differential equations in radius, which may contain up to fourth order derivatives, after separation of the time dependence. In applications small magnetic, viscous or thermal diffusion may lead to boundary layers of second or higher order. We investigate key aspects of the discretisation of the radial equations using one dimensional hp-finite element methods through two model problems: reduction of order versus higher order elements for an ordinary differential equation of fourth order; and fourth order boundary layers. Results indicate that

higher order elements are to be favoured over a reduction of order, and that robust exponential convergence may be achieved for the symmetric two layer problem investigated.

Contents

1 Introduction

We consider the discretisation of the incompressible magnetohydrodynamic (MHD) equations, linearised about a steady basic state in spherical geometries. Poloidal-toroidal representations are used for the velocity and magnetic field. The angular dependence is discretised using a Galerkin method: the basic state is expanded in vector spherical harmonics and the perturbation toroidal and poloidal potentials, and the temperature are expanded in spherical harmonics. This produces a coupled system of ordinary differential equations in radius, which may contain up to fourth order derivatives, after separation of the time

dependence. Previously the radial dependence has been discretised using finite differences [2] or Chebychev collocation. However, one dimensional hp-finite element (FE) methods are of present interest, since they lead to practical exponential convergence in problems with boundary layers [8, §3.4, e.g.] (§3). In order to apply hp-FE methods to the coupled systems, it is first necessary to find out which method of approach to a fourth order equation should be employed, reduction of order (§2.1), or a higher order expansion (§2.2). Reduction of order for the h-version FE method has been treated before [6, 7], and higher order expansions are mentioned [8], but here we present a side by side comparison for the hp-FE method (§2.3). Numerical results indicate that a higher order expansion achieves faster convergence rates (Figure 2). For boundary layers, we investigate a fourth order problem. Now there is an extra inner layer to resolve, that distinguishes this problem from that studied by Schwab [8, §3.4]. The numerical results indicate exponential convergence (Figure 4), which has been observed for a range of values a and d determining the thicknesses of the layers.

1.1 The magnetohydrodynamic equations

The incompressible MHD equations for an electrically-conducting Boussinesq fluid are linearised about a steady basic state $(\mathbf{v}_0, \mathbf{B}_0, \Theta_0)$. In a frame rotating with uniform angular velocity $\boldsymbol{\Omega}$ the perturbation velocity $\mathbf{v}'$, magnetic induction $\mathbf{B}'$ and temperature Θ' are governed [2, 3] by

$$\begin{aligned}
\rho(\partial_t - \nu\nabla^2)\mathbf{v}' &= -\rho(\boldsymbol{\omega}_0 \times \mathbf{v}' + \boldsymbol{\omega}' \times \mathbf{v}_0 + 2\boldsymbol{\Omega} \times \mathbf{v}') \\
&\quad - \nabla P' + \mathbf{J}_0 \times \mathbf{B}' + \mathbf{J}' \times \mathbf{B}_0 - \rho\alpha_\Theta \Theta' \mathbf{g}_e \,, \qquad (1) \\
(\partial_t - \eta\nabla^2)\mathbf{B}' &= \nabla \times (\mathbf{v}_0 \times \mathbf{B}') + \nabla \times (\mathbf{v}' \times \mathbf{B}_0) \,, \qquad (2) \\
(\partial_t - \kappa\nabla^2)\Theta' &= -\mathbf{v}_0 \cdot \mathbf{q}' - \mathbf{v}' \cdot \mathbf{q}_0 + Q'/\rho c_p \\
&\quad + 2\nu(\nabla \mathbf{v}_0)_S : (\nabla \mathbf{v}')_S / c_p + 2\mathbf{J}_0 \cdot \mathbf{J}'/\sigma\rho c_p \,, \qquad (3)
\end{aligned}$$

where $P' := p' + \rho \mathbf{v}_0 \cdot \mathbf{v}'$, $\mathbf{q}_0 := \nabla\Theta_0$, $\mathbf{q}' := \nabla\Theta'$ and $\mathbf{g}_e := -\nabla U_e$ with the effective gravitational potential $U_e := U - \frac{1}{2}(\boldsymbol{\Omega} \times \mathbf{r})^2$. Further, the following

solenoidal conditions hold,

$$\nabla \cdot \mathbf{v}' = 0\,, \quad \nabla \cdot \mathbf{B}' = 0\,. \tag{4}$$

1.2 Solution in spherical geometries

Equations (4) in spherical geometries are satisfied by the solenoidal toroidal-poloidal representations, $\mathbf{B}' = \mathbf{T}\{T'\} + \mathbf{S}\{S'\}$ and $\mathbf{v} = \mathbf{T}\{t'\} + \mathbf{S}\{s'\}$, where toroidal and poloidal fields are defined by $\mathbf{T}\{T\} := \nabla \times \{T\mathbf{r}\}$ and $\mathbf{S}\{S\} := \nabla \times \nabla \times \{S\mathbf{r}\}$ with potentials T and S and radial vector $\mathbf{r}$.

Equations (1)–(3) are satisfied by a Galerkin method in the spherical polar angles [3], expanding the perturbation scalar fields in spherical harmonics, $f = \sum_\alpha f_\alpha Y_\alpha$ for $f = S', T', s', t', P', \Theta', U_e$, and the basic state vector fields in vector spherical harmonics, $\mathbf{F} = \sum_\alpha F_\alpha \mathbf{Y}_\alpha$ for $\mathbf{F} = \mathbf{B}_0, \mathbf{J}_0, \mathbf{v}_0, \boldsymbol{\omega}_0, \mathbf{q}_0, \mathbf{g}_e$. Greek subscripts and superscripts denote multi-indices [3].

The Galerkin method yields the t'_γ, s'_γ, S'_γ, T'_γ, Θ'_γ equations,

$$\begin{aligned}(\partial_t - \nu D_\gamma) t'_\gamma = \sum_{\alpha,\beta} \Big\{ &- (\omega^0_\alpha \nu'_\beta \nu'_\gamma) + (\nu^0_\alpha \omega'_\beta \nu'_\gamma) + \rho^{-1}(J^0_\alpha B'_\beta \nu'_\gamma) \\ &- \rho^{-1}(B^0_\beta J'_\alpha \nu'_\gamma) - \alpha_\Theta (g^e_\alpha \Theta'_\beta \nu'_\gamma) - 2(\Omega_\alpha \nu'_\beta \nu'_\gamma) \Big\}\,, \end{aligned} \tag{5}$$

$$\begin{aligned}(\partial_t - \nu D_\gamma D_\gamma) s'_\gamma = \sum_{\alpha,\beta,\gamma_1} \Big\{ &- (\omega^0_\alpha \nu'_\beta \nu'_\gamma) + (\nu^0_\alpha \omega'_\beta \nu'_\gamma) + \rho^{-1}(J^0_\alpha B'_\beta \nu'_\gamma) \\ &- \rho^{-1}(B^0_\beta J'_\alpha \nu'_\gamma) - \alpha_\Theta (g^e_\alpha \Theta'_\beta \nu'_\gamma) - 2(\Omega_\alpha \nu'_\beta \nu'_\gamma) \Big\}\,, \end{aligned} \tag{6}$$

$$(\partial_t - \eta D_\gamma) S'_\gamma = \sum_{\alpha,\beta} \Big\{ (\nu^0_\alpha B'_\beta B'_\gamma) - (B^0_\alpha \nu'_\beta B'_\gamma) \Big\}\,, \tag{7}$$

$$(\partial_t - \eta D_\gamma) T'_\gamma = \sum_{\alpha,\beta,\gamma_1} \Big\{ (\nu^0_\alpha B'_\beta B'_\gamma) - (B^0_\alpha \nu'_\beta B'_\gamma) \Big\}\,, \tag{8}$$

$$(\partial_t - \kappa D_\gamma) \Theta'_\gamma = \frac{Q'_\gamma}{\rho c_p} - \sum_{\alpha,\beta} \Big\{ (\nu^0_\alpha q'_\beta \Theta'_\gamma) + (q^0_\alpha \nu'_\beta \Theta'_\gamma) - \nu c_p^{-1} (\nu^0_\alpha \nu'_\beta \Theta'_\gamma) \tag{9}$$

$$- (\mu_0 \sigma \rho c_p)^{-1} (J^0_\alpha J_\beta \Theta'_\gamma) \Big\} , \tag{10}$$

where $D_\gamma := \partial_{rr} + 2r^{-1}\partial_r - \gamma(\gamma+1)r^{-2}$ and $r = |\mathbf{r}|$. A typical interaction term is $(\omega^0_\alpha \nu'_\beta \nu'_\gamma) :=$

$$e_\nu(\gamma) f_\nu(\beta) (\mathbf{Y}_\alpha \times \mathbf{Y}_\beta, \mathbf{Y}_\gamma) \begin{cases} \partial^\gamma(\omega^0_\alpha \partial_\beta s'_\beta), & \gamma_1 = \gamma \pm 1, \beta_1 = \beta \pm 1; \\ \partial^\gamma(\omega^0_\alpha t'_\beta), & \gamma_1 = \gamma \pm 1, \beta_1 = \beta; \\ \omega^0_\alpha \partial_\beta s'_\beta, & \gamma_1 = \gamma, \beta_1 = \beta \pm 1; \\ \omega^0_\alpha t'_\beta, & \gamma_1 = \gamma, \beta_1 = \beta; \end{cases}$$

where the angular dependence is contained in the coupling integral

$$(\mathbf{Y}_\alpha \times \mathbf{Y}_\beta, \mathbf{Y}_\gamma) := \frac{1}{4\pi} \oint \mathbf{Y}_\alpha \times \mathbf{Y}_\beta \cdot \mathbf{Y}^*_\gamma \, d\Omega ,$$

$d\Omega := \sin\theta \, d\theta \, d\phi$, $\partial^\gamma := \partial_r + \gamma^* r^{-1}$, and $\partial_\gamma := \partial_r + \gamma_* r^{-1}$ with γ^* and γ_* constants dependent on γ. The other interaction terms have similar expressions [3].

In equations (5)–(10) the s'_γ-equation is fourth order in r; the remaining equations are second order. The diffusion parameters ν, η and κ, which multiply the highest r-derivatives in each equation, may be very small in applications and hence produce boundary layers. Lastly, for steady basic states, steady or eigenvalue solutions may be determined.

2 Systems of mixed order

From the previous section, the equations of interest (5)–(10) are coupled systems of ordinary differential equations, up to degree four. The fourth order terms may be handled in essentially two ways, and to compare these we consider the simple problem: find $y \in C^4[a, b]$ such that

$$y^{(4)} = f , \tag{11}$$

$$y(a) = Y_a\,, \quad y(b) = Y_b\,, \tag{12}$$
$$y'(a) = Y'_a\,, \quad y'(b) = Y'_b\,, \tag{13}$$

where Y_a, Y_b, Y'_a and Y'_b are given real numbers. This is equivalent to a simple static Euler–Bernoulli beam equation [5, 1]. Although a simple model problem, by suitable choice of f (one that is difficult to approximate by polynomials, for example an oscillatory function), the convergence of the two methods are compared in §2.3 to determine the method to use in practice.

2.1 Method 1: coupled second order system

The first method involves rewriting the fourth order equation as a coupled second order system. Let $z = y''$ and rewrite (11) as

$$z'' = f\,, \quad y'' - z = 0\,.$$

Now multiplying these equations by the test functions ϕ_0 and ϕ_1, respectively, adding, and integrating over the domain $[a, b]$,

$$(z'\phi_0 + y'\phi_1)\Big|_a^b - \int_a^b (z'\phi_0' + y'\phi_1' + z\phi_1)\,dx = \int_a^b f\phi_0\,dx\,.$$

The known values of $y'(a)$ and $y'(b)$, may be included in the weak form by choosing $\phi_1 \in H^1$. As the values $z'(a)$ and $z'(b)$ are unknown, take $\phi_0 \in H^1_0$, where $H^1_0 = \{\lambda \in H^1 \mid \lambda(a) = \lambda(b) = 0\}$. Finally, write $y = y_h + y_b$, where $y_h \in H^1_0$, and y_b is a known function (that will be written in terms of the finite element basis functions) that satisfies (12). Upon rearranging, the resulting weak form is

$$\int_a^b (z'\phi_0' + y_h'\phi_1' + z\phi_1)\,dx = Y'_b\phi_1(b) - Y'_a\phi_1(a) - \int_a^b (y_b'\phi_1' + f\phi_0)\,dx\,.$$

From this weak form a matrix system is constructed, by expanding the test and trial functions in terms of basis functions ψ_j^i on element i. These

basis functions are generated from the basis functions ψ_j on the standard element $[-1,1]$. One such hierarchical basis is

$$\psi_1(\xi) = \tfrac{1}{2}(1-\xi)\,, \quad \psi_2(\xi) = \tfrac{1}{2}(1+\xi)\,, \quad \psi_n(\xi) = (1-\xi^2)P^{1,1}_{n-3}(\xi)\,,\ n>2\,,$$

where ψ_1 and ψ_2 are boundary modes and ψ_n, $n>2$, are interior modes. Here $P^{\alpha,\beta}_n(\xi)$ refers to the unnormalized Jacobi polynomial of degree n corresponding to the weight function $(1-\xi)^\alpha(1+\xi)^\beta$ where $\alpha,\beta > -1$ [4, Appendix A]. The interior modes can be normalised [8, §3.1.4], so that $\int_{-1}^{1}(\psi_n')^2\,d\xi = 1$. The first four modes are plotted in Figure 1(a).

The stiffness matrix is assembled element-wise in the usual way, after applying static condensation of the interior modes [8, 4]. Care must be exercised in the overlapping of blocks (to enforce continuity).

2.2 Method 2: one higher order system

A higher order (C^1) expansion is used. Multiplying equation (11) by the test function ϕ, and integrating over $[a,b]$,

$$(y^{(3)}\phi)\Big|_a^b - \int_a^b y^{(3)}\phi'\,dx = \int_a^b f\phi\,dx\,.$$

Choosing $\phi \in H^2_0 = \{\lambda \in H^2 \mid \lambda(a) = \lambda(b) = \lambda'(a) = \lambda'(b) = 0\}$, and integrating by parts again results in the following weak form

$$\int_a^b y_h''\phi''\,dx = \int_a^b (f\phi - y_b''\phi'')\,dx\,,$$

where $y = y_h + y_b$, but now $y_h \in H^2_0$ and y_b satisfies (12) and (13). The matrix system is formed by again expanding in terms of basis functions ψ^i_j on element i. A hierarchical basis ψ_j, suitable for a C^1 expansion, is defined on the standard element $[-1,1]$ by

$$\psi_1(\xi) = \tfrac{1}{4}(1-\xi)^2(2+\xi)\,, \quad \psi_2(\xi) = \tfrac{1}{4}(1-\xi)^2(1+\xi)\,,$$

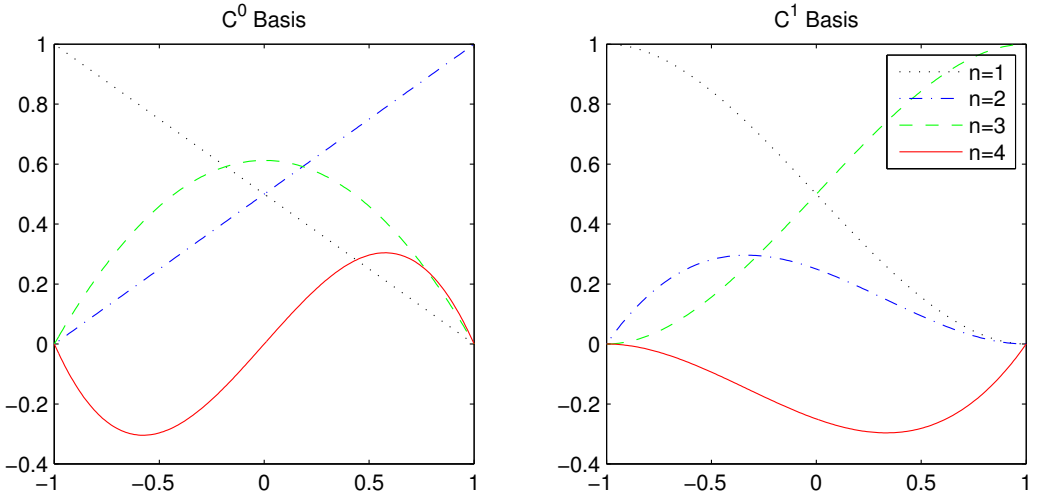

FIGURE 1: (a) C^0 and (b) C^1 hierarchical basis functions $\psi_n(\xi)$.

$$\psi_3(\xi) = \tfrac{1}{4}(1+\xi)^2(2-\xi)\,, \quad \psi_4(\xi) = -\tfrac{1}{4}(1+\xi)^2(1-\xi)\,,$$
$$\psi_n(\xi) = (1-\xi^2)^2 P^{2,2}_{n-5}(\xi)\,,\ n>4\,.$$

In this case there are four boundary modes, ψ_n, $1 \leqslant n \leqslant 4$. The ψ_1 and ψ_3 are used to enforce continuity, and ψ_2 and ψ_4, the continuity of the derivative. The interior modes ψ_n, $n>4$, can be normalised [8, §3.1.4] so that $\int_{-1}^{1}(\psi_n'')^2\,d\xi = 1$. The boundary modes are plotted in Figure 1(b).

For an expansion $y = \sum_{i,j} y_j^i \psi_j^i(x)$, where $\psi_j^i(x) = \psi_j(\chi_i^{-1}(x))$ and $\xi = \chi_i^{-1}(x) = (2x - x_i - x_{i+1})/h_i$ with $h_i = x_{i+1} - x_i$, the continuity of y' implies $y'(x_{i+1}^-) = y'(x_{i+1}^+)$, or $y_4^i/h_i = y_2^{i+1}/h_{i+1}$. This condition may be enforced by taking terms $h_i\psi_2^i(x)$ and $h_i\psi_4^i(x)$ in the expansion for y. This certainly simplifies the assembly of the stiffness matrix (condensed blocks from adjacent elements are overlapped, in this case 2×2 blocks). If the neighbouring mesh widths, h_i, are of similar order, this works well. In the boundary layer problems considered in the next section, the neighbouring h_is vary significantly in order of magnitude. The terms $h_i\psi_2^i(x)$ and $h_i\psi_4^i(x)$

then produce scaling issues in the assembled stiffness matrix.

By instead taking terms $\max(h_{i-1}, h_i)\psi_2^i(x)$ and $\max(h_i, h_{i+1})\psi_4^i(x)$ in the expansion for y, and modifying the assembly appropriately, 2×2 blocks may still be overlapped without producing scaling issues. This also means that any symmetry of the problem is preserved (against, say, introducing extra equations for the continuity of the derivative).

2.3 Method 2 versus method 1

The two methods have been tested for an oscillatory right hand side $f = A\sin(\alpha x - \beta)$ where A, α and β are constants, by p-refinement on a ten element uniform mesh of $[0, 1]$, for various values of Y_0, Y_1, Y_0' and Y_1'. The results indicate much faster convergence for the higher order method, a typical plot is shown in Figure 2. The relative error in the L^2 norm between the hp-FE solution (or derivatives) calculated from either method 1 or 2, and the exact solution (or derivatives) is plotted against the degrees of freedom. The L^2 norm is chosen for ease of calculation.

3 Fourth order boundary layers

For the second order boundary layer problem

$$-d^2u'' + u = 1\,, \quad u(\pm 1) = 0\,, \tag{14}$$

where $d \ll 1$, Schwab [8] shows that the three element mesh-degree combination $\{-1, -1 + \kappa\tilde{n}d, 1 - \kappa\tilde{n}d, 1\}$, $(n, 1, n)$, where $\tilde{n} = n + 1/2$ and κ is a constant which may be taken as one, gives exponential convergence. Moreover, the convergence is uniform with respect to d in the energy norm defined by

$$\|u\|_d^2 = \int_{-1}^{1} \left(d^2(u')^2 + u^2\right)\, dx\,.$$

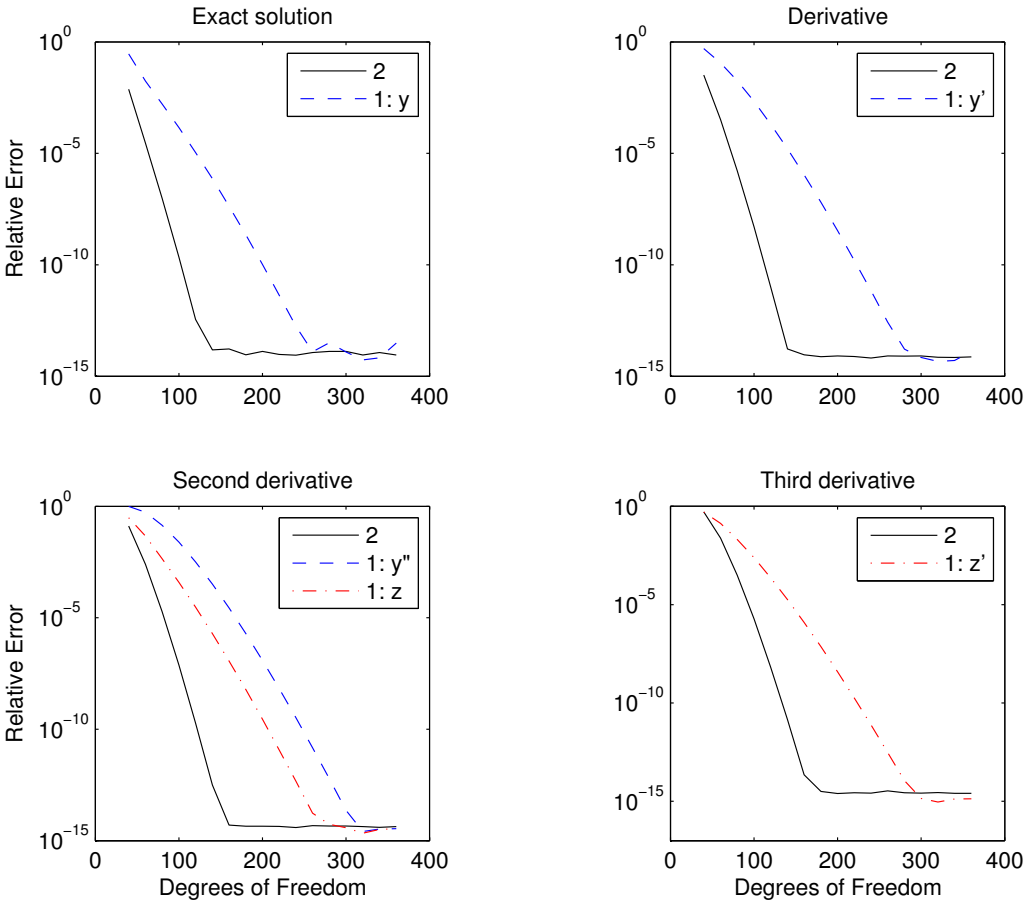

FIGURE 2: Relative errors in solution (or derivatives) of (11) versus number of degrees of freedom, for $f = (6\pi)^{-4}\sin(6\pi x - \frac{1}{3})$, on $[0,1]$, $y(0) = y'(0) = y'(1) = 0$, $y(1) = 1$.

This three element mesh-degree combination is employed for values of n and d outside the super-exponential convergence range of the one element p-version. This range occurs when $r = e/(2\tilde{n}d) < 1$. The analysis by Schwab [8] shows that for these values of r, the error in the energy norm of the p-version is bounded by $Cd^{1/2}r^{\tilde{n}}(1-r^2)^{-1/2}$, where C is independent of n and d. The interior solution is resolved by the one element of fixed order. If the right-hand side of the differential equation in (14) was not one (or a polynomial for that matter), then the overall convergence rate would depend on the approximation of the smoother components in the solution (the part of the exact solution separate from the boundary layer components) [8, §3.4.4, Remark 3.56].

As the equations of interest contain terms up to fourth order, it is of interest to determine whether the results obtained by Schwab [8] for the second order case can be extended to a fourth order example. In order to do this consider the following problem

$$(ad^2)^2u^{(4)} - (1+a^2)d^2u'' + u = 1\,, \quad u(\pm 1) = 0\,, \quad u'(\pm 1) = 0\,, \qquad (15)$$

where $0 < a < 1$ determines the relative boundary layer thickness. Thus, for this problem there is an inner boundary layer of thickness ad, contained in an outer boundary layer of thickness d, and an interior region. The presence of the inner boundary layer distinguishes this problem from that studied by Schwab [8]. For this equation, we have the weak form,

$$B(u,\phi) = \int_{-1}^{1} \left[(ad^2)^2u''\phi'' + (1+a^2)d^2u'\phi' + u\phi\right]\,dx = \int_{-1}^{1} f\phi\,dx\,,$$

where $\phi \in H_0^2$, (and $f = 1$ in our case) and the corresponding energy norm,

$$\|u\|_d^2 = B(u,u) = \int_{-1}^{1} \left[(ad^2)^2(u'')^2 + (1+a^2)d^2(u')^2 + u^2\right]\,dx\,.$$

The relative error in the energy norm between the exact solution u and the calculated solution $\tilde{u}$ is

$$E_R(a,d)^2 = \frac{B(u-\tilde{u},u-\tilde{u})}{B(u,u)} = \frac{B(u,u)+B(\tilde{u},\tilde{u})-2B(u,\tilde{u})}{B(u,u)}$$

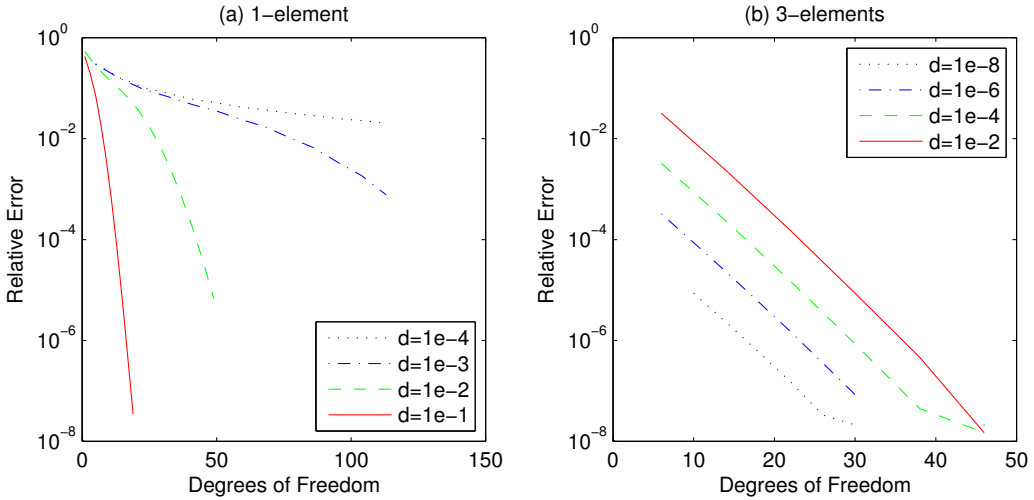

FIGURE 3: Relative errors in solution of (15) versus number of degrees of freedom for (a) the one element p version and (b) the three element hp version, with $a = 0.9$.

$$= 1 - \frac{\int_{-1}^{1} \tilde{u} f \, dx}{\int_{-1}^{1} u f \, dx},$$

after simplifying, using that u satisfies (15) and that $B(u, u) = (u, f)$, $B(\tilde{u}, \tilde{u}) = (\tilde{u}, f)$, where $(\cdot, \cdot)$ is the L^2 inner product on $[-1, 1]$.

For our particular case, from the exact form of the solution one obtains that

$$(u, 1) = 2 - \frac{2d(1 - a^2)\tanh[1/(ad)]\tanh(1/d)}{\tanh[1/(ad)] - a\tanh(1/d)}.$$

Firstly, we note that when a is close to one, the boundary layer components are essentially the same (the inner layer thickness approaches the outer layer thickness). Therefore, the fourth order problem is approximated by a

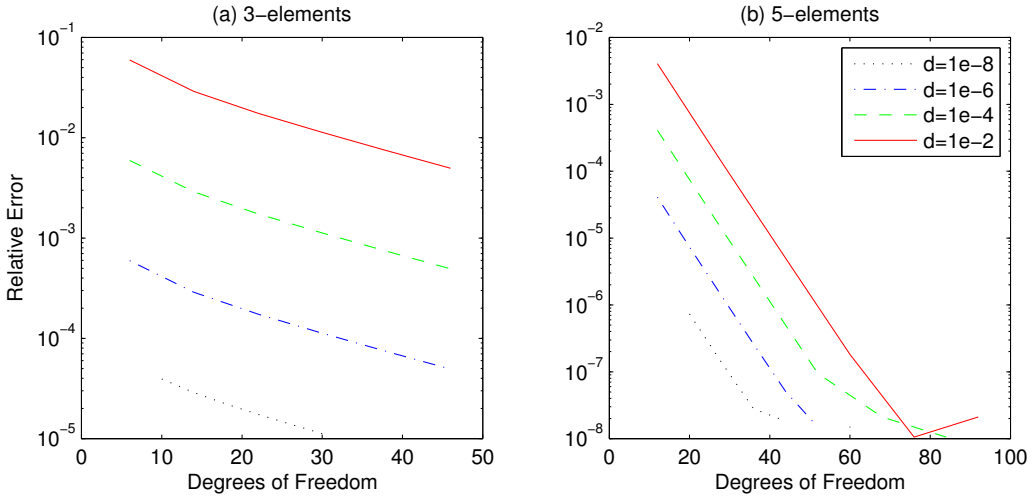

FIGURE 4: Relative errors in solution of (15) versus number of degrees of freedom for (a) the three element mesh and (b) the five element mesh, with $\mathfrak{a} = 0.1$ and $\mathfrak{d} = 10^{-2}, 10^{-4}, 10^{-6}, 10^{-8}$.

second order problem. We expect the three element mesh-degree combination to produce similar convergence results as observed for the second order problem (14) [8, §3.4.7]. This is indeed the case, as Figures 3(a) and 3(b) illustrate for a range of $\mathfrak{d}$ values.

As can be seen in Figure 3(a), for larger values of $\mathfrak{d}$ the $\mathfrak{p}$-version converges rapidly, but as $\mathfrak{d}$ decreases, more degrees of freedom are required to reach the super-exponential convergence range. In contrast, for the three element mesh, this behaviour is reversed: the *smaller* the value of $\mathfrak{d}$, the *faster* the convergence. This rather surprising behaviour is observed for the second order problem (14), consistent with the analytical bounds on the relative error in the energy norm, derived by Schwab [8, §3.4].

Our primary interest is in what happens as $\mathfrak{a}$ decreases, say $\mathfrak{a} = 0.1$. For this value of $\mathfrak{a}$, observe in Figure 4(a) a deterioration in the convergence

results for the three element mesh, as the inner boundary layer is no longer resolved. We still observe faster convergence for smaller d values, but the rate is no longer exponential. Using the three element result for the second order boundary layer problem as a guide, we propose the following five element mesh-degree combination

$$\{-1, -1 + \tilde{n}ad, -1 + \tilde{n}d, 1 - \tilde{n}d, 1 - \tilde{n}ad, 1\}, \quad (n, n, 3, n, n),$$

that is, we insert an extra element of the same width as the thickness of the inner layer. With this extra element, we expect to resolve the inner boundary layer as a becomes small, producing better convergence results than for the three element version. Figure 4(b) illustrates the five element mesh for $a = 0.1$. For this smaller value of a the five element method achieves exponential convergence in the relative energy norm, with faster convergence the smaller the value of d.

4 Conclusions and future research

We observed that for fourth order equations a higher order expansion gives much faster convergence rates than a coupled system of lower order equations.

For the fourth order boundary layer example, the proposed five element mesh-degree combination gives exponential convergence when $a \ll 1$ (we tested the result with a as small as 10^{-6}). Numerical experiments indicate that the three element mesh-degree combination should be used when $0.4 < a < 1$. We anticipate that the method will work well for higher order problems, by adding further elements of width proportional to the thickness of the layer. In applications the solution in the interior may require more than one element of fixed order for exponential convergence.

Some of the steps towards the solution of the full system, (5)–(10), requiring further research are: investigation of the convergence of eigensolutions of the discretised linearised MHD equations (and hence the linear stability of

non-linear solutions); the influence of the coordinate singularity at $r = 0$; matching conditions across material boundaries; and the infinite interval problem for the exterior.

References

[1] A. Ghali and A. M. Neville. *Structural Analysis: a unified classical and matrix approach*. E & Fn Spon, London; New York, 1997. C384

[2] D. J. Ivers and C. G. Phillips. A vector spherical harmonic spectral code for linearised magnetohydrodynamics. *ANZIAM J.*, 44(E):C423–C442, 2003. http://anziamj.austms.org.au/ojs/index.php/ANZIAMJ/article/view/689 C381

[3] D. J. Ivers and C. G. Phillips. Scalar and vector spherical harmonic spectral equations of rotating magnetohydrodynamics. *Geophysical Journal International*, 175:955–974, 2008. doi:10.1111/j.1365-246X.2008.03944.x C381, C382, C383

[4] George Em Karniadakis and Spencer Sherwin. *Spectral hp Element Methods for Computational Fluid Dynamics*, Second Edition. Oxford University Press, Oxford, 2005. doi:10.1093/acprof:oso/9780198528692.001.0001 C385

[5] P. K. Kythe and D. Wei. *An introduction to linear and nonlinear finite element analysis, A computational approach*. Birkhäuser Boston, Inc., Boston, MA, 2004. doi:10.1115/1.1818688 C384

[6] T. Miyoshi. A finite element method for the solutions of fourth order partial differential equations. *Kumamoto Journal of Science*, 9:87–116, 1972/73. C381

[7] M. Mori. *The Finite Element Method and its Applications,* Translated from the Japanese. MacMillan Co., New York, 1986. C381

[8] C. Schwab. *p- and hp-Finite Element Methods, Theory and Applications in Solid and Fluid Mechanics*. Oxford University Press, Oxford, 1998. C381, C385, C386, C387, C389, C391

Author addresses

1. **D. Farmer**, School of Mathematics and Statistics, University of Sydney, Sydney, New South Wales 2006, Australia.
mailto:davidf@maths.usyd.edu.au

2. **D. J. Ivers**, School of Mathematics and Statistics, University of Sydney, Sydney, New South Wales 2006, Australia.
mailto:david.ivers@sydney.edu.au